



ELSEVIER

Contents lists available at ScienceDirect

Metabolic Engineering

journal homepage: www.elsevier.com/locate/ymben

Metabolic network reconstruction, growth characterization and ^{13}C -metabolic flux analysis of the extremophile *Thermus thermophilus* HB8

Aditi Swarup¹, Jing Lu¹, Kathleen C. DeWoody, Maciek R. Antoniewicz*

Department of Chemical & Biomolecular Engineering, Metabolic Engineering and Systems Biology Laboratory, University of Delaware, Newark DE 19716, USA

ARTICLE INFO

Article history:

Received 9 April 2014

Received in revised form

3 May 2014

Accepted 20 May 2014

Available online 5 June 2014

Keywords:

Extremophile

Thermophilic bacterium

Optimal growth

Metabolic network model

Isotopic labeling

ABSTRACT

Thermus thermophilus is an extremely thermophilic bacterium with significant biotechnological potential. In this work, we have characterized aerobic growth characteristics of *T. thermophilus* HB8 at temperatures between 50 and 85 °C, constructed a metabolic network model of its central carbon metabolism and validated the model using ^{13}C -metabolic flux analysis (^{13}C -MFA). First, cells were grown in batch cultures in custom constructed mini-bioreactors at different temperatures to determine optimal growth conditions. The optimal temperature for *T. thermophilus* grown on defined medium with glucose was 81 °C. The maximum growth rate was 0.25 h⁻¹. Between 50 and 81 °C the growth rate increased by 7-fold and the temperature dependence was described well by an Arrhenius model with an activation energy of 47 kJ/mol. Next, we performed a ^{13}C -labeling experiment with [1,2- ^{13}C] glucose as the tracer and calculated intracellular metabolic fluxes using ^{13}C -MFA. The results provided support for the constructed network model and highlighted several interesting characteristics of *T. thermophilus* metabolism. We found that *T. thermophilus* largely uses glycolysis and TCA cycle to produce biosynthetic precursors, ATP and reducing equivalents needed for cells growth. Consistent with its proposed metabolic network model, we did not detect any oxidative pentose phosphate pathway flux or Entner-Doudoroff pathway activity. The biomass precursors erythrose-4-phosphate and ribose-5-phosphate were produced via the non-oxidative pentose phosphate pathway, and largely via transketolase, with little contribution from transaldolase. The high biomass yield on glucose that was measured experimentally was also confirmed independently by ^{13}C -MFA. The results presented here provide a solid foundation for future studies of *T. thermophilus* and its metabolic engineering applications.

© 2014 International Metabolic Engineering Society. Published by Elsevier Inc. All rights reserved.

1. Introduction

Thermus thermophilus is an extremely thermophilic aerobic bacterium that has become an important model organism for structural biology studies and has significant biotechnological potential (Cava et al., 2009). Currently, two genome sequences are available for *T. thermophilus* strains HB8 and HB27 (Bruggemann and Chen, 2006; Henne et al., 2004). In the late 1990s, an international initiative was started at the RIKEN Genomic Sciences Center in Japan with the goal of determining the 3D-structures of all predicted proteins in *T. thermophilus* (Yokoyama et al., 2000a, 2000b), and recently, an even

more ambitious project was initiated, the “Structural and Functional Whole-Cell Project for *T. thermophilus* HB8”, with the goal of “understanding the mechanisms of all biological phenomena occurring in *T. thermophilus* HB8” (www.thermus.org). As a result of these large-scale efforts, *T. thermophilus* HB8 is currently one of the best known organisms from a structural point of view. More than 20% of its encoded proteins have rendered 3D structures.

In addition to structural biology investigations, *T. thermophilus* is now also being considered as a potential host organism for biotechnological applications (Cava et al., 2009; Henne et al., 2004). With its high growth rate, high cell yield, and most importantly the constitutive expression of an efficient natural competence system, *T. thermophilus* stands out among the thermophiles as a potential candidate host for metabolic engineering programs (Averhoff and Muller, 2010; Cava et al., 2009). However, surprisingly little is known about its growth characteristics and metabolism. Without this baseline of information, further studies

* Correspondence to: Department of Chemical and Biomolecular Engineering, University of Delaware 150 Academy St, Newark, DE 19716, USA.
Fax: +302 831 1048.

E-mail address: mranton@udel.edu (M.R. Antoniewicz).

¹ These authors contributed equally to this work.

that focus on identifying metabolic bottlenecks, engineering metabolic pathways and rewiring fluxes cannot proceed.

Thus, the main goal of this study was to establish this basic knowledge for *T. thermophilus*. First, we investigated cell growth of *T. thermophilus* HB8 in batch cultures using a minimum medium with glucose as the only carbon source. From a series of growth experiments we determined the optimal growth medium, growth temperature and maximum growth rate. Next, we constructed a metabolic network model of *T. thermophilus* central carbon metabolism, based on the available literature data, and validated the model using ^{13}C -metabolic flux analysis (^{13}C -MFA). The flux analysis results provided new and interesting insights into the metabolism of this extremely thermophilic bacterium. In summary, this study provides the first rigorous characterization of the metabolism of *T. thermophilus* and lays the foundation for future metabolic engineering applications on this organism.

2. Materials and methods

2.1. Materials and growth medium

Media and chemicals were purchased from Sigma-Aldrich (St. Louis, MO). [1,2- ^{13}C]Glucose (99+ atom% ^{13}C) was purchased from Cambridge Isotope Laboratories (Andover, MA). Wolfe's minerals (Cat. No. MD-TMS) and Wolfe's vitamins (Cat. No. MD-VS) were purchased from ATCC (Manassas, VA), and Tris solution was purchased from Cellgro (Cat. No. 46-031-CM). Glucose stock solutions were prepared at 20 wt% in distilled water. The optimized minimum medium contained (per liter of medium): 0.50 g K_2HPO_4 , 0.30 g KH_2PO_4 , 0.50 g NH_4Cl , 0.50 g NaCl , 0.20 g $\text{MgCl}_2 \cdot 6\text{H}_2\text{O}$, 0.04 g $\text{CaSO}_4 \cdot 2\text{H}_2\text{O}$, 40 mL of 1 M Tris, 5 mL of Wolfe's minerals, and 5 mL of Wolfe's vitamins. The pH of the medium was 7.9. The optimized medium used in this study is largely based on medium described by Yoshida et al. (1984). All media and stock solutions were sterilized by filtration.

2.2. Strain and growth conditions

T. thermophilus HB8 (ATCC 27634, Manassas, VA) was grown aerobically in mini-bioreactors with a working volume of 10 mL. The culture vessels were 15-mL Hungate tubes (Bellco Glass Cat. No. 2047-16125). Each tube had a screw cap with a rubber septum that was pierced by three needles for: (i) supply of filter-sterilized air; (ii) sampling of cell culture; and (iii) venting of off-gasses. The mini-bioreactors were autoclaved before inoculation. A high-precision multichannel peristaltic pump (Watson Marlow, Wilmington, MA) was used to control the air flow to the mini-bioreactors, which was set at 11.3 mL/min. Evaporation losses were prevented by using water-saturated air for aeration, i.e. by first bubbling the air through distilled water at 70 °C. Gas flow rates were monitored by a digital flow-meter (Supelco, Veri-Flow 500). Mixing in the mini-bioreactors was achieved through the rising gas bubbles, and the temperature was maintained constant by placing the tubes in a dry heating block (Fisher Isotemp Digital Dry-Bath 125D).

For growth experiments and the ^{13}C -tracer experiment, cells from a frozen stock were first pre-cultured at 70 °C to early exponential growth. The cells were then used to inoculate a new culture at the indicated growth temperature. The defined medium contained 18 mM glucose and the initial OD_{600} was 0.015. For the ^{13}C -tracer experiment at 70 °C, the defined medium contained 9 mM of [1,2- ^{13}C]glucose and the initial OD_{600} was about 0.015. The tracer [1,2- ^{13}C]glucose was chosen because it allows good resolution of metabolic fluxes in central carbon metabolism in microbes (He et al., 2014).

2.3. Analytical methods

Medium samples were collected during the exponential growth phase and at the end of the growth phase. Biomass concentration was determined by measuring the optical density at 600 nm (OD_{600}) using a spectrophotometer (Eppendorf BioPhotometer), and assuming 0.39 (g/L)/ OD_{600} cell dry weight and 25.3 g/C-mol for the molecular weight of dry biomass (Antoniewicz et al., 2007c). After centrifugation, the supernatant was separated from the biomass pellet and glucose concentration in the supernatant was determined by YSI 2700 biochemistry analyzer (YSI, Yellow Springs, OH). Concentrations of by-products of metabolism in the supernatant were determined using an Agilent 1200 Series HPLC. Biomass pellets were stored at -80 °C prior to GC-MS analysis.

2.4. Determination of specific growth rate

Growth rates were determined from the measured biomass time course data and glucose time course data. To model cell growth, the following two differential equations were used, which describe the evolution of biomass (x) and glucose concentration (s) in batch culture (Ahn and Antoniewicz, 2013):

$$\frac{dx}{dt} = \mu x \quad (1)$$

$$\frac{ds}{dt} = -\frac{dx}{dt} \frac{1}{Y_{sx}} = -\frac{\mu}{Y_{sx}} x \quad (2)$$

Here, μ is the specific growth rate, and Y_{sx} is the yield of biomass on glucose. Integration of Eqs. (1) and (2) yields:

$$x(t) = x_0 \exp(\mu t) \quad (3)$$

$$s(t) = s_0 - \frac{x_0}{Y_{sx}} [\exp(\mu t) - 1] \quad (4)$$

Eqs. (3) and (4) can be rearranged such that they can be used to estimate the specific growth rate by linear regression of biomass and glucose concentrations over time (here, subscript '0' denotes initial concentrations):

$$\ln(x) = \ln(x_0) + \mu t \quad (5)$$

$$\ln\left((s_0 - s) \frac{Y_{sx}}{x_0} + 1\right) = \mu t \quad (6)$$

2.5. GC-MS analysis of proteinogenic amino acids

GC-MS analysis of *tert*-butyldimethylsilyl (TBDMS) derivatized proteinogenic amino acids was performed as described previously (Leighty and Antoniewicz, 2012). GC-MS analysis was performed on an Agilent 7890A GC system equipped with a DB-5MS capillary column (30 m, 0.25 mm i.d., 0.25 μm -phase thickness; Agilent J&W Scientific), connected to a Waters Quattro Micro Tandem Mass Spectrometer (GC-MS/MS) operating under ionization by electron impact (EI) at 70 eV. Helium flow was maintained at 1.0 mL/min via electronic pressure control. The source temperature was maintained at 200 °C, and interface temperature at 250 °C. The temperature of the column was started at 80 °C for 2 min, increased to 280 °C at 7 °C/min and held for 20 min. Mass spectra were recorded in selected ion recording (SIR) mode with 30 ms dwell time. Mass isotopomer distributions were obtained by integration of ion chromatograms (Antoniewicz et al., 2007a), and corrected for natural isotope abundances (Fernandez et al., 1996).

2.6. GC–MS analysis of glucose

Labeling of glucose in the medium was determined by GC–MS analysis of the aldonitrile pentapropionate derivative of glucose (Antoniewicz et al., 2011). For GC–MS analysis, 10 μL of medium sample was derivatized as described previously (Antoniewicz et al., 2011). The injection volume was 1 μL and samples were injected at 1:40 split ratio. Helium flow was maintained at 1.0 mL/min. The injection port temperature was 250 $^{\circ}\text{C}$. The temperature of the column was started at 80 $^{\circ}\text{C}$ for 1 min, increased to 280 $^{\circ}\text{C}$ at 15 $^{\circ}\text{C}/\text{min}$, and held for 6 min. Labeling of glucose was determined from the mass isotopomer distribution of the fragment at m/z 370, which contains carbon atoms C1–C5 of glucose (Antoniewicz et al., 2011).

2.7. Metabolic network model

A metabolic network model of *T. thermophilus* central carbon metabolism was constructed for ^{13}C -MFA based on KEGG and PathwayTools metabolic pathway databases (Caspi et al., 2012; Kanehisa and Goto, 2000; Kanehisa et al., 2012). The model includes all major metabolic pathways of central carbon metabolism. A lumped biomass reaction (v_{41}) was used to describe the drain of precursor metabolites and co-factors required for cell growth. The complete model is provided in Appendix A.

2.8. ^{13}C -Metabolic flux analysis

^{13}C -MFA was performed using the Metran software (Crown and Antoniewicz, 2013b; Yoo et al., 2008), which is based on the elementary metabolite units (EMU) framework (Antoniewicz et al., 2007b; Young et al., 2008). Fluxes were estimated by minimizing the variance-weighted sum of squared residuals (SSR) between the experimentally measured and model predicted mass isotopomer distributions of amino acids using non-linear least-squares regression (Antoniewicz et al., 2006). Flux estimation was repeated 10 times starting with random initial values for all fluxes to find a global solution. At convergence, accurate 95% confidence intervals were computed for all estimated fluxes by evaluating the sensitivity of the minimized SSR to flux variations (Antoniewicz et al., 2006). Precision of estimated fluxes was determined as follows (Antoniewicz et al., 2006):

$$\text{Flux precision (stdev)} = [(\text{flux}_{\text{upper bound 95\%}}) - (\text{flux}_{\text{lower bound 95\%}})] / 4 \quad (7)$$

To describe the fractional labeling of biomass amino acids, G-value parameters were included in ^{13}C -MFA. One G-value parameter was included for each measured amino acid, as described previously (Antoniewicz et al., 2007c; Leighty and Antoniewicz, 2012). Reversible reactions were modeled as separate forward and backward fluxes. Net and exchange fluxes were determined as follows: $v_{\text{net}} = v_f - v_b$; $v_{\text{exch}} = \min(v_f, v_b)$.

2.9. Goodness-of-fit analysis

To determine the goodness-of-fit, the ^{13}C -MFA fitting result was subjected to a χ^2 -statistical test. In short, assuming the model is correct and data are without gross measurement errors, the minimized SSR is a stochastic variable with a χ^2 -distribution. The number of degrees of freedom is equal to the number of fitted measurements n minus the number of estimated independent parameters p . The acceptable range of SSR values is between $\chi^2_{\alpha/2}(n-p)$ and $\chi^2_{1-\alpha/2}(n-p)$, where α is a certain chosen threshold value, for example 0.05 for 95% confidence interval (Antoniewicz et al., 2006).

3. Results and discussion

3.1. Cell growth at different temperatures

First, we investigated optimal growth conditions for *T. thermophilus* HB8 on minimum medium with glucose as the only carbon source. For this purpose, the medium described by Yoshida et al. (Yoshida et al., 1984) was optimized to achieve reproducible growth characteristics for *T. thermophilus* HB8 in batch cultures with 3 g/L of glucose. All growth experiments were performed in custom-constructed mini-bioreactors with 10-mL working volume at temperatures between 50 and 85 $^{\circ}\text{C}$. To maintain a constant culture temperature, the culture tubes were placed in a dry heating block. We confirmed that the temperature in the liquid was uniform. We also accounted for potential heat losses to the surrounding by directly measuring the temperature of the medium. At 50 $^{\circ}\text{C}$ setting, the temperature of the medium was very

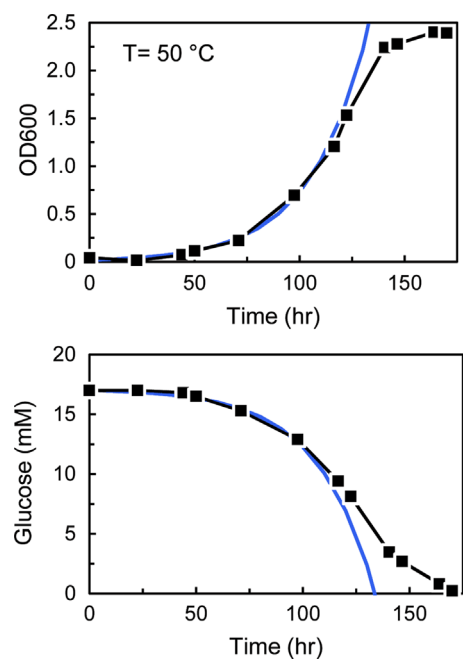


Fig. 1. Representative growth profile of *T. thermophilus* HB8 grown at 50 $^{\circ}\text{C}$. The blue solid line represents the predicted cell growth and glucose profile for an estimated growth rate of 0.037 h^{-1} .

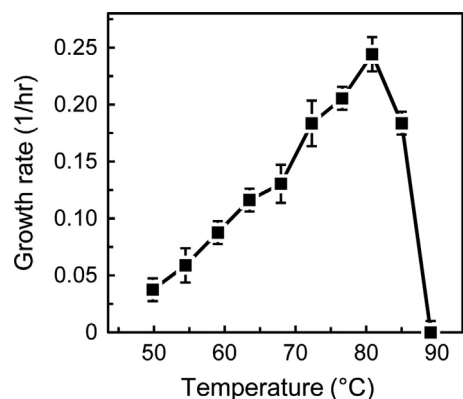


Fig. 2. Specific growth rates of *T. thermophilus* HB8 grown on minimum medium with 3 g/L glucose as the only carbon source at different temperatures. The error bars represent the span of growth rates estimated by regression of biomass data and glucose time course data.

to 0.25 h^{-1} . The growth rate decreased to 0.18 h^{-1} at $85 \text{ }^\circ\text{C}$, and no growth was observed at $90 \text{ }^\circ\text{C}$, or higher temperatures. Thus, in our experimental setup, the maximum growth rate for *T. thermophilus* HB8 was 0.25 h^{-1} and the optimum growth temperature was $81 \text{ }^\circ\text{C}$. The increase in growth rate between 50 and $81 \text{ }^\circ\text{C}$ was described well by an Arrhenius type model with an activation

energy of 47 kJ/mol :

$$\mu(1/h) = 0.24 \exp\left[\frac{47,000}{R}\left(\frac{1}{353} - \frac{1}{273+T}\right)\right] \quad (8)$$

Similar Arrhenius activation energies were measured for other microbes (Huang et al., 2011).

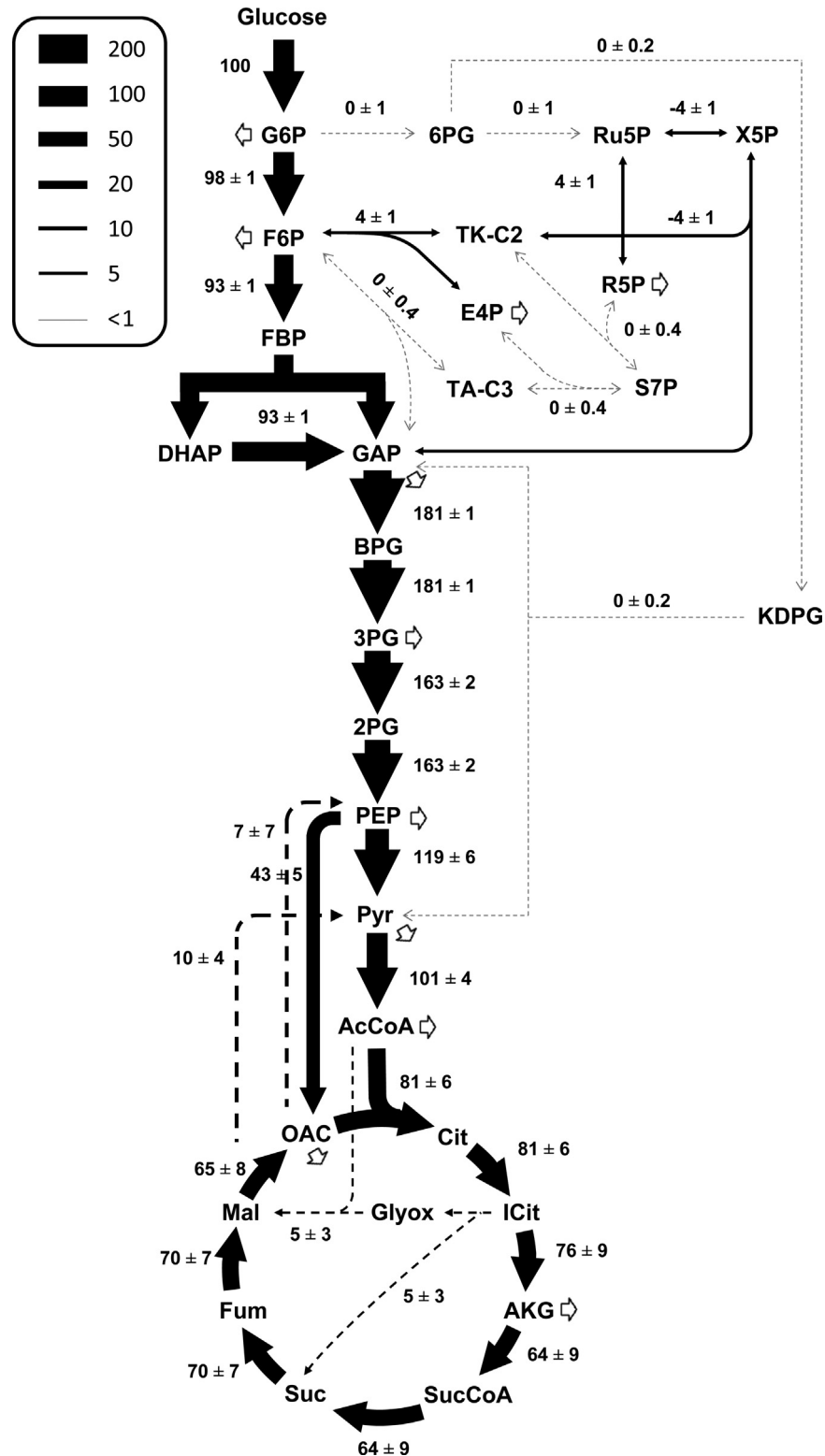


Fig. 4. Metabolic flux distributions in central metabolic pathways of *T. thermophilus* HB8 during exponential growth on minimum medium at $70 \text{ }^\circ\text{C}$. Fluxes were determined by ^{13}C -MFA and are shown here normalized to glucose uptake rate of 100 (estimated flux \pm SD). Dashed lines denote fluxes for which the 95% confidence interval included a zero flux value.

3.2. ^{13}C -Metabolic flux analysis and network model validation

A metabolic network model of *T. thermophilus* central carbon metabolism was constructed for ^{13}C -MFA based on the KEGG and BioCyc databases. The model contained all major metabolic pathways of central carbon metabolism, which had been annotated, and also included several pathways that had been hypothesized to be absent in *T. thermophilus* (e.g. oxidative pentose phosphate pathway and Entner-Doudoroff pathway). We expected that ^{13}C -MFA would provide support for these hypotheses. The complete model, which contains 41 reactions, is given in Appendix A and is shown schematically in Fig. 3. ^{13}C -MFA was performed with this model using isotopic-labeling data from the [1,2- ^{13}C] glucose tracer experiment. Metabolic fluxes were determined by fitting the measured mass isotopomer distributions for seven fragments of the amino acids alanine, aspartate, and glutamate (Supplementary Materials, Table S1), which are directly derived from pyruvate, oxaloacetate and α -ketoglutarate, respectively. In total, 36 mass isotopomer measurements were fitted to estimate 10 independent free fluxes, 2 exchange fluxes and 3 G-value parameters. Thus, there were 21 redundant measurements in this analysis. We obtained a statistically acceptable fit, assuming 0.3 mol% measurement errors for all GC-MS measurements. The minimized SSR value of 26 was lower than the maximum statistically acceptable SSR value of 35 at 95% confidence level with 21 degrees of freedom.

The estimated metabolic fluxes are shown schematically in Fig. 4. The complete flux results are shown in Supplementary Materials (Table S2). *T. thermophilus* catabolized glucose almost exclusively via glycolysis and TCA cycle. Consistent with its hypothesized metabolic model, the oxidative pentose phosphate pathway (v_9 , $v_{10}=0\pm 1$) and Entner-Doudoroff pathway (v_{18} , $v_{19}=0.0\pm 0.2$) were determined to carry no flux. The biomass precursors erythrose-4-phosphate and ribose-5-phosphate were produced via the non-oxidative pentose phosphate pathway reactions, and largely via transketolase (v_{13} , $v_{14}=4\pm 1$) with little or no contribution from transaldolase (v_{16} , $v_{17}=0\pm 0.4$). Several other reactions also determined to carry no significant flux, defined here as fluxes for which the 95% confidence interval included a zero flux value, including glyoxylate shunt (v_{29} , $v_{30}=5\pm 3$); malic enzyme (v_{31} , $v_{32}=5\pm 4$); and the flux from oxaloacetate to phosphoenolpyruvate ($v_{34}=7\pm 7$). A large fraction of the pyruvate formed via glycolysis was catabolized in the TCA cycle, which resulted in relatively high TCA cycle fluxes. As an example, the citrate synthase flux ($v_{21}=81\pm 6$) was about five times higher in *T. thermophilus* than in *Escherichia coli* grown on glucose in batch culture (17 ± 0.3 , (Leighty and Antoniewicz, 2013)).

The measured biomass yield was not employed as a constraint in ^{13}C -MFA; instead, it was estimated by ^{13}C -MFA and then compared to the measured value. The estimated biomass flux of $v_{17}=3.64\pm 0.18$ corresponds to a biomass yield of 0.51 ± 0.03 g dry weight per gram glucose. This is significantly higher than the measured biomass yield of 0.33 ± 0.02 g dry weight per gram glucose. There are several possible explanations for this discrepancy. First, we noted that *T. thermophilus* had a tendency to form biofilms on the glass and needles in our culture experiments. Thus, the measured biomass yield based on liquid phase measurements almost certainly underestimated the true biomass yield. Second, the lumped biomass equation that was used in ^{13}C -MFA to describe growth of *T. thermophilus* was based on limited available literature data. A better characterization of biomass composition for *T. thermophilus* could provide an improved estimate of the true biomass flux using ^{13}C -MFA. Third, it is possible that *T. thermophilus* produced by-products that we did not detect. We used HPLC to measure common by-products of metabolism (e.g. acetate, lactate, and ethanol); however, we did not detect any significant

amounts of these products in the supernatant. Perhaps *T. thermophilus* produced some volatile by-products that evaporated at our high-temperature culture conditions, and therefore we did not detect them by HPLC.

4. Conclusions

In this work, we have provided the first detailed characterization of the growth physiology and metabolism of *T. thermophilus* HB8 on minimum medium. We determined that *T. thermophilus* has a wide effective growth temperature range spanning more than 35 °C, between 50 and 85 °C. Under our culture conditions, the optimal growth temperature was 81 °C, which is slightly higher than previously reported for this organism (Cava et al., 2009; Nordstrom and Laakso, 1992; Sakaki and Oshima, 1975). When the cells were grown between 50 and 81 °C, the growth rate increased continually, and this was captured accurately by an Arrhenius model with an activation energy of 47 kJ/mol. The high biomass yield on glucose, estimated to be between 0.33 and 0.51 g_{DW}/g, is indicative of efficient metabolism of this organism. As an example, the biomass yield is similar to that of *E. coli* grown on minimum medium with glucose (0.36 g_{DW}/g, (Leighty and Antoniewicz, 2012)); it is higher than that of the thermophilic bacterium *Geobacillus thermoglucosidasius* ($T_{\text{opt}}=60$ °C; biomass yield= 0.27 ± 0.05 g_{DW}/g, (Tang et al., 2009)), and similar to the biomass yield of the strict aerobe *Pseudomonas sp.* (biomass yield= 0.64 ± 0.01 g_{DW}/g, (Lang et al., 2014)). The growth rate of *T. thermophilus* (0.25 h^{-1}) is similar to that of *G. thermoglucosidasius* ($0.31\pm 0.04\text{ h}^{-1}$), and slightly lower compared to *Pseudomonas sp.* ($0.41\pm 0.01\text{ h}^{-1}$). All of these results support the significant potential of *T. thermophilus* for biotechnological applications.

With the baseline knowledge established in this study, future research on *T. thermophilus* should focus on establishing an improved metabolic model that includes secondary metabolic pathways (Tang et al., 2012). We plan to utilize the power of parallel labeling experiments (Crown and Antoniewicz, 2013a; Crown et al., 2011) and tandem mass spectrometry (Antoniewicz, 2013b; Choi and Antoniewicz, 2011; Choi et al., 2012) to further improve the model and quantify dynamics of metabolic fluxes in batch and fed-batch cultures using recently developed dynamic metabolic flux analysis (DMFA) techniques (Antoniewicz, 2013a; Leighty and Antoniewicz, 2011).

Acknowledgments

This work was supported by NSF MCB-1120684 grant.

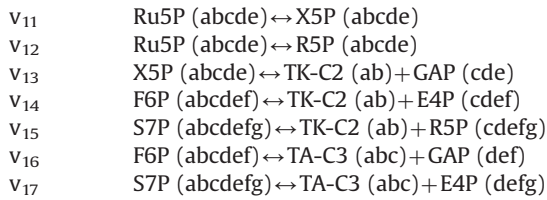
Appendix A. Metabolic network model of *T. thermophilus* for ^{13}C metabolic flux analysis

Glycolysis

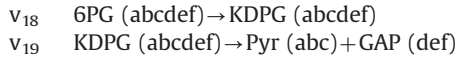
v_1	Gluc.ext (abcdef)+ATP→G6P (abcdef)
v_2	G6P (abcdef)↔F6P (abcdef)
v_3	F6P (abcdef)+ATP→FBP (abcdef)
v_4	FBP (abcdef)↔DHAP (cba)+GAP (def)
v_5	DHAP (abc)↔GAP (abc)
v_6	GAP (abc)↔3PG (abc)+ATP+NADH
v_7	3PG (abc)↔PEP (abc)
v_8	PEP (abc)→Pyr (abc)+ATP

Pentose Phosphate Pathway

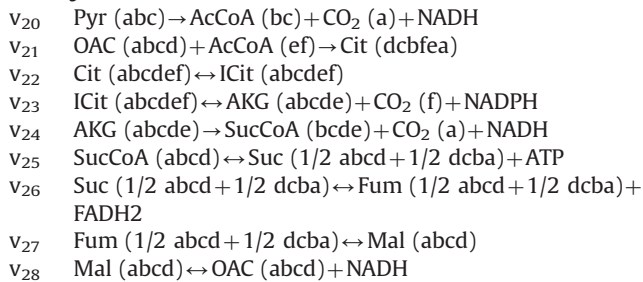
v_9	G6P (abcdef)→6PG (abcdef)+NADPH
v_{10}	6PG (abcdef)→Ru5P (bcdef)+CO ₂ (a)+NADPH



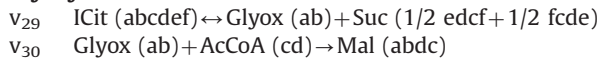
Entner-Doudoroff Pathway



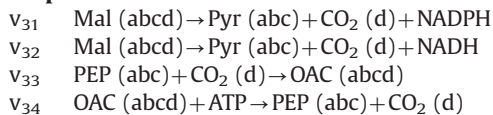
TCA Cycle



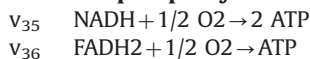
Glyoxylate Shunt



Amphibolic reactions



Oxidative phosphorylation



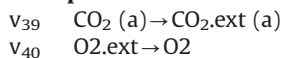
Transhydrogenation



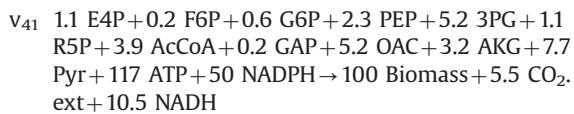
ATP hydrolysis



Transport



Biomass formation



Appendix B. Supporting information

Supplementary data associated with this paper can be found in the online version at <http://dx.doi.org/10.1016/j.jymben.2014.05.013>.

References

- Ahn, W.S., Antoniewicz, M.R., 2013. Parallel labeling experiments with [1,2-(13)C] glucose and [U-(13)C]glutamine provide new insights into CHO cell metabolism. *Metab. Eng.* 15, 34–47.
 Antoniewicz, M.R., 2013a. Dynamic metabolic flux analysis-tools for probing transient states of metabolic networks. *Curr. Opin. Biotechnol.* 24, 973–978.
 Antoniewicz, M.R., 2013b. Tandem mass spectrometry for measuring stable-isotope labeling. *Curr. Opin. Biotechnol.* 24, 48–53.

- Antoniewicz, M.R., Kelleher, J.K., Stephanopoulos, G., 2006. Determination of confidence intervals of metabolic fluxes estimated from stable isotope measurements. *Metab. Eng.* 8, 324–337.
 Antoniewicz, M.R., Kelleher, J.K., Stephanopoulos, G., 2007a. Accurate assessment of amino acid mass isotopomer distributions for metabolic flux analysis. *Anal. Chem.* 79, 7554–7559.
 Antoniewicz, M.R., Kelleher, J.K., Stephanopoulos, G., 2007b. Elementary metabolite units (EMU): a novel framework for modeling isotopic distributions. *Metab. Eng.* 9, 68–86.
 Antoniewicz, M.R., Kelleher, J.K., Stephanopoulos, G., 2011. Measuring deuterium enrichment of glucose hydrogen atoms by gas chromatography/mass spectrometry. *Anal. Chem.* 83, 3211–3216.
 Antoniewicz, M.R., Kraynie, D.F., Laffend, L.A., Gonzalez-Lergier, J., Kelleher, J.K., Stephanopoulos, G., 2007c. Metabolic flux analysis in a nonstationary system: fed-batch fermentation of a high yielding strain of *E. coli* producing 1,3-propanediol. *Metab. Eng.* 9, 277–292.
 Averhoff, B., Muller, V., 2010. Exploring research frontiers in microbiology: recent advances in halophilic and thermophilic extremophiles. *Res. Microbiol.* 161, 506–514.
 Bruggemann, H., Chen, C., 2006. Comparative genomics of *Thermus thermophilus*: plasticity of the megaplasmid and its contribution to a thermophilic lifestyle. *J. Biotechnol.* 124, 654–661.
 Caspi, R., Altman, T., Dreher, K., Fulcher, C.A., Subhraveti, P., Keseler, I.M., Kothari, A., Krummenacker, M., Latendresse, M., Mueller, L.A., Ong, Q., Paley, S., Pujar, A., Shearer, A.G., Travers, M., Weerasinghe, D., Zhang, P., Karp, P.D., 2012. The MetaCyc database of metabolic pathways and enzymes and the BioCyc collection of pathway/genome databases. *Nucleic Acids Res.* 40, D742–D753.
 Cava, F., Hidalgo, A., Berenguer, J., 2009. *Thermus thermophilus* as biological model. *Extremophiles* 13, 213–231.
 Choi, J., Antoniewicz, M.R., 2011. Tandem mass spectrometry: a novel approach for metabolic flux analysis. *Metab. Eng.* 13, 225–233.
 Choi, J., Grossbach, M.T., Antoniewicz, M.R., 2012. Measuring complete isotopomer distribution of aspartate using gas chromatography/tandem mass spectrometry. *Anal. Chem.* 84, 4628–4632.
 Crown, S.B., Antoniewicz, M.R., 2013a. Parallel labeling experiments and metabolic flux analysis: past, present and future methodologies. *Metab. Eng.* 16, 21–32.
 Crown, S.B., Antoniewicz, M.R., 2013b. Publishing 13C metabolic flux analysis studies: a review and future perspectives. *Metab. Eng.* 20, 42–48.
 Crown, S.B., Indurthi, D.C., Ahn, W.S., Choi, J., Papoutsakis, E.T., Antoniewicz, M.R., 2011. Resolving the TCA cycle and pentose-phosphate pathway of *Clostridium acetobutylicum* ATCC 824: isotopomer analysis, in vitro activities and expression analysis. *Biotechnol. J.* 6, 300–305.
 Fernandez, C.A., Des Rosiers, C., Previs, S.F., David, F., Brunengraber, H., 1996. Correction of 13C mass isotopomer distributions for natural stable isotope abundance. *J. Mass Spectrom.* 31, 255–262.
 He, Xiao, Gebreselassie, Zhang, Antoniewicz, Tang and Peng, Central metabolic responses to the overproduction of fatty acids in *Escherichia coli* based on C-metabolic flux analysis. *Biotechnol. Bioeng.* 2014 111, 575–585.
 Henne, A., Bruggemann, H., Raasch, C., Wiezer, A., Hartsch, T., Liesegang, H., Johann, A., Lienard, T., Gohl, O., Martinez-Arias, R., Jacobi, C., Starkuviene, V., Schlenczek, S., Dencker, S., Huber, R., Klenk, H.P., Kramer, W., Merkl, R., Gottschalk, G., Fritz, H.J., 2004. The genome sequence of the extreme thermophile *Thermus thermophilus*. *Nat. Biotechnol.* 22, 547–553.
 Huang, L., Hwang, A., Phillips, J., 2011. Effect of temperature on microbial growth rate-mathematical analysis: the Arrhenius and Eyring–Polanyi connections. *J. food Sci.* 76, E553–E560.
 Kanehisa, M., Goto, S., 2000. KEGG: kyoto encyclopedia of genes and genomes. *Nucleic Acids Res.* 28, 27–30.
 Kanehisa, M., Goto, S., Sato, Y., Furumichi, M., Tanabe, M., 2012. KEGG for integration and interpretation of large-scale molecular data sets. *Nucleic Acids Res.* 40, D109–D114.
 Lang, K., Zierow, J., Buehler, K., Schmid, A., 2014. Metabolic engineering of *Pseudomonas* sp. strain VLB120 as platform biocatalyst for the production of isobutyric acid and other secondary metabolites. *Microb. Cell Fact.* 13, 2.
 Leighty, R.W., Antoniewicz, M.R., 2011. Dynamic metabolic flux analysis (DMFA): a framework for determining fluxes at metabolic non-steady state. *Metab. Eng.* 13, 745–755.
 Leighty, R.W., Antoniewicz, M.R., 2012. Parallel labeling experiments with [U-(13)C] glucose validate *E. coli* metabolic network model for (13)C metabolic flux analysis. *Metab. Eng.* 14, 533–541.
 Leighty, R.W., Antoniewicz, M.R., 2013. COMPLETE-MFA: complementary parallel labeling experiments technique for metabolic flux analysis. *Metab. Eng.* 20, 49–55.
 Nordstrom, K.M., Laakso, S.V., 1992. Effect of growth temperature on fatty acid composition of ten thermus strains. *Appl. Environ. Microbiol.* 58, 1656–1660.
 Sakaki, Y., Oshima, T., 1975. Isolation and characterization of a bacteriophage infectious to an extreme thermophile, *Thermus thermophilus* HB8. *J. Virol.* 15, 1449–1453.
 Tang, J.K., You, L., Blankenship, R.E., Tang, Y.J., 2012. Recent advances in mapping environmental microbial metabolisms through 13C isotopic fingerprints. *J. R. Soc., Interface* 9, 2767–2780.
 Tang, Y.J., Sapra, R., Joyner, D., Hazen, T.C., Myers, S., Reichmuth, D., Blanch, H., Keasling, J.D., 2009. Analysis of metabolic pathways and fluxes in a newly discovered thermophilic and ethanol-tolerant *Geobacillus* strain. *Biotechnol. Bioeng.* 102, 1377–1386.
 Yokoyama, K., Ohkuma, S., Taguchi, H., Yasunaga, T., Wakabayashi, T., Yoshida, M., 2000. V-Type H⁺-ATPase/synthase from a thermophilic eubacterium, *Thermus*

- thermophilus. Subunit structure and operon. *J. Biol. Chem.* 275, 13955–13961.
- Yokoyama, S., Hirota, H., Kigawa, T., Yabuki, T., Shirouzu, M., Terada, T., Ito, Y., Matsuo, Y., Kuroda, Y., Nishimura, Y., Kyogoku, Y., Miki, K., Masui, R., Kuramitsu, S., 2000b. Structural genomics projects in Japan. *Nat. Struct. Biol.* 7, 943–945.
- Yoo, H., Antoniewicz, M.R., Stephanopoulos, G., Kelleher, J.K., 2008. Quantifying reductive carboxylation flux of glutamine to lipid in a brown adipocyte cell line. *J. Biol. Chem.* 283, 20621–20627.
- Yoshida, T., Lorence, R.M., Choc, M.G., Tarr, G.E., Findling, K.L., Fee, J.A., 1984. Respiratory proteins from the extremely thermophilic aerobic bacterium, *Thermus thermophilus*. *J. Biol. Chem.* 259, 112–123.
- Young, J.D., Walther, J.L., Antoniewicz, M.R., Yoo, H., Stephanopoulos, G., 2008. An elementary metabolite unit (EMU) based method of isotopically nonstationary flux analysis. *Biotechnol. Bioeng.* 99, 686–699.